Geophys. J. Int. (2004) **158,** 489–505 doi: 10.1111/j.1365-246X.2004.02329.x

The Matuyama–Brunhes boundary interval (500–900 ka) in North Atlantic drift sediments

J. E. T. Channell,[1] J. H. Curtis[1] and B. P. Flower[2]

[1]*Department of Geological Sciences,* PO Box 112120, *University of Florida, Gainesville,* FL 32611, *USA. E-mail: jetc@nersp.nerdc.ufl.edu*
[2]*College of Marine Science, University of South Florida, St Petersburg,* FL 33701, *USA*

Accepted 2004 April 4. Received 2004 March 12; in original form 2002 October 28

SUMMARY

Ocean Drilling Program (ODP) sites 984 and 983, located on North Atlantic sediment drifts, provide high-resolution records across the Matuyama–Brunhes boundary. At ODP site 984 (Bjorn Drift, Iceland Basin), the mean sedimentation rate in the 500–900 ka interval is ~12 cm kyr^{-1} based on an age model derived by matching the planktonic and benthic oxygen isotope records to an Ice Volume Model. The Matuyama–Brunhes polarity transition at site 984, as defined by virtual geomagnetic polar (VGP) latitudes <50°, has an apparent duration of ~7 kyr with a mid-point at 773.5 ka, compared with 772.5 ka at neighbouring site 983. Outside the polarity transition at both sites 984 and 983, excursions in VGP latitudes, to values <20°, at 540, 590 and 670 ka correspond to troughs in the palaeointensity record.

New u-channel palaeomagnetic data across the Matuyama–Brunhes boundary, for working and archive halves of core sections from three holes at both sites 984 and 983, augment data published by Channell & Lehman (1997) and are compared with back-to-back 1 cm^3 discrete samples. Clusters of VGPs in the South Atlantic and northeast Asia in both u-channel and discrete sample records imply that polarity transition fields have characteristics similar to the modern non-axial-dipole (NAD) field.

Key words: geomagnetic reversals, magnetostratigraphy, Matuyama–Brunhes boundary, palaeointensity.

1 INTRODUCTION

An important stimulus for the detailed study of polarity reversals was the observation that virtual geomagnetic poles (VGPs) at Plio-Pleistocene polarity reversals tend to be longitudinally confined to the Americas (~60°W) or Australia/eastern Asia (~120°E) (Clement 1991; Laj *et al.* 1991). This confinement was related to heterogeneous lowermost mantle structure, indicated by seismic tomography (e.g. Dziewonski 1984), and the influence of lower-mantle heterogeneity on core convection.

In the Matuyama–Brunhes boundary (MBB) database of Love & Mazaud (1997), the authors selected 11 volcanic and sedimentary records as acceptable, based on sampling and measurement procedure and the characteristics of the records themselves. Volcanic rocks yield instantaneous (unsmoothed) but discontinuous records of polarity reversals, and the relative age of individual flows is difficult to estimate within a few thousand years using available radiometric methods. This is a major drawback when the process being studied (polarity reversal) has a duration of a few thousand years. Sedimentary records have more predictable, but not assured, continuity but may be more influenced by artefacts attributable to remanence acquisition, sampling and measurement procedure. Only three of the 11 records in the MBB database of Love & Mazaud (1997) are from deep-sea marine sediments. These three records are from Deep Sea Drilling Project (DSDP) hole 609B in the North Atlantic (Clement & Kent 1987), DSDP hole 664D in the equatorial Atlantic (Valet *et al.* 1989) and core V16-58 in the Indian Ocean (Clement & Kent 1991). For these three records, sedimentation rates across the boundary are estimated to be 6 cm kyr^{-1}, 3 cm kyr^{-1} and 4 cm kyr^{-1} respectively. These records were among the higher-sedimentation-rate records documenting the preferred longitudes of VGP paths at polarity transitions (Clement 1991; Laj *et al.* 1991).

Some high-sedimentation-rate (~10 cm kyr^{-1}) polarity transition records yield VGP paths that are distinctly different from the longitudinally constrained paths seen in lower-sedimentation-rate records (Channell & Lehman 1997; Oda *et al.* 2000). In the higher-sedimentation-rate records, the VGPs are not longitudinally confined and jump abruptly between VGP clusters which, in some cases, have a similar location to the VGP clusters observed from volcanic records (Hoffman 1992). This has led to the supposition that the longitudinally constrained VGP paths are at least partly a result of the smoothing affect of low sedimentary accumulation rates (Channell & Lehman 1997). The observed VGP clusters seen in some volcanic and sedimentary data are located off South America, in North America, off Australia and in northeast Asia, coinciding

with radial flux centres at the Earth's surface in today's non-axial dipole (NAD) field (Hoffman 1992, 2000).

The generally accepted astrochronological age (780 ka) for the MBB was derived using the Ice Volume Model (Imbrie & Imbrie 1980) as a tuning target for the oxygen isotope data from Ocean Drilling Program (ODP) site 677 (Shackleton *et al.* 1990). Magnetic polarity stratigraphy was not resolved at site 677; therefore, the age of the MBB (and other Matuyama polarity reversals) was determined by correlation of the ODP site 677 isotope stratigraphy to magnetic/isotope stratigraphies from DSDP sites 552 and 607. The mean sedimentation rate at ODP site 677 over the last 1 Myr is ∼4 cm kyr^{-1}. The high mean sedimentation rates at ODP site 984 (∼12 cm kyr^{-1}) provide an opportunity to match isotope and palaeomagnetic records from the same cores across the MBB at higher resolution than has been possible previously. To produce the site 984 age model, we matched the site 984 oxygen isotope records to the Ice Volume Model (Imbrie & Imbrie 1980), computed using the summer insolation at 65°N from Berger & Loutre (1991), and compared the precession component derived from the two signals.

Geomagnetic palaeointensity records from North and South Atlantic sediment-drift sites indicate that they are, at least for the last glacial cycle, largely controlled by the global-scale field and can be used for sub-Milankovitch-scale correlation (e.g. Laj *et al.* 2000; Stoner *et al.* 2002). Numerical modelling of palaeointensity records with different mean sedimentation rates and variable-quality age control indicates that drift sedimentation rates (>5 cm kyr^{-1}) and high-quality isotopic age control are necessary to reliably capture the variability of palaeointensity (Guyodo & Channell 2002). In addition to these conditions, for the normalization procedure to produce reliable palaeointensity proxies the magnetic remanence should be carried by fine-grained pseudo-single-domain (PSD) or single-domain (SD) magnetite and magnetic concentration parameters should vary by less than an order of magnitude (King *et al.* 1983; Tauxe 1993). This latter restriction is based on the fact that larger changes in concentration give non-linear behaviour in ARM normalization. These conditions appear to be fulfilled at sites 984 and 983, and therefore the palaeointensity records from these two sites are compared in the 500–900 ka interval spanning the MBB.

2 ODP SITES 983 AND 984

ODP site 984 (61.43°N, 24.08°W) is located on the Bjorn Drift in the Iceland Basin (Fig. 1) and was occupied in July 1995 during ODP leg 162. The site is 116 km from ODP site 983, located on the Gardar Drift. The magnetic polarity stratigraphies at ODP sites 984 and 983 have been documented from spaced 7 cm^3 discrete samples and from shipboard pass-through magnetometer data (Channell & Lehman 1999). For sites 984 and 983, the polarity record extends back to the Réunion Subchron (∼2.2 Ma) and the Olduvai Subchron (∼1.9 Ma) respectively.

The published u-channel records from site 983/984 polarity transitions comprise two from the MBB at site 983, three from the MBB at site 984, three from the top of the Jaramillo Subchronozone at site 983 (Channell & Lehman 1997) and one from the top of the Olduvai Subchronozone at site 983 (Mazaud & Channell 1999). Integrated palaeomagnetic and isotopic records are available for the last 500 kyr from sites 983 and 984 (Channell 1999). The pre-500 ka palaeomagnetic and isotopic record at site 983 has been documented for the 725–1150 ka interval (Channell & Kleiven 2000) and the 500–725 ka interval (Channell *et al.* 1998). The latter paper dealt with the palaeointensity record only, and not with the directional palaeomagnetic record. The site 983/984 directional and palaeointensity records have been compared for the 0.9–2.2 Ma interval by Channell *et al.* (2002). In addition to the palaeomagnetic/isotopic studies cited above, ODP leg 162 sites from the Iceland Basin (sites 980–984) have produced other Quaternary palaeoceanographic and magnetic records (Raymo *et al.* 1998; Oppo *et al.* 1998; McIntyre *et al.* 1999; McManus *et al.* 1999; Venz *et al.* 1999; Flower *et al.* 2000; Kleiven *et al.* 2003; Channell & Raymo 2003; Channell *et al.* 2003).

Here we document the oxygen isotope data and the magnetic directional and palaeointensity records for the 500–900 ka interval from site 984, and compare them with the published data from site 983 (Channell *et al.* 1998; Channell & Kleiven 2000). Magnetic data have been generated from u-channel samples that have a 2 × 2 cm square cross-section, are up to 1.5 m in length and provide a means of continuous subsampling of the sedimentary section (Tauxe *et al.* 1983). Pass-through magnetometers designed for u-channel samples (Weeks *et al.* 1993) allow magnetic remanence measurements to be made at centimetre increments down-core, although the response function of the pick-up coils (width ∼4 cm, see Guyodo *et al.* 2002) means that adjacent measurements at spacings of <4 cm are not independent.

The majority of u-channels for this study were collected from the archive halves of the site 983/984 composite sections. The composite section is the optimal splice from the (four) holes drilled at the site (see Hagelberg *et al.* 1992) constructed on-board ship from magnetic susceptibility, gamma-ray attenuation porosity (GRAPE) and colour reflectance data (Shipboard Scientific Party 1996). The process results in a composite section calibrated in metres composite depth (mcd). The MBB polarity transition was recorded in both working and archive halves from several holes at sites 983 and 984, allowing the reproducibility of the transition record to be assessed. New u-channel records augment those presented by Channell & Lehman (1997), and u-channel records from holes 983B, 983C and 984A are compared with data from 1 cm^3 discrete cubic samples collected back-to-back from alongside the u-channel samples.

3 ISOTOPE DATA

At site 984 planktonic oxygen isotope measurements were carried out on monospecific samples of *Neogloboquadrina pachyderma* (sinistral) selected from the 212–300 μm size fraction. Benthic oxygen isotope measurements were made on benthic foraminifera, using specimens of *Cibicidoides wuellerstorfi* and *C. kullenbergi* selected from the >150 μm size fraction. Low abundance of these two species led us to augment the benthic record with samples of *Cassidulina*. The benthic data were analysed at the University of California, Santa Cruz, while the planktonic record was measured at the University of Florida. A few benthic data points across the marine isotope stage (MIS) 19/20 transition were generated at the University of Florida. Samples were reacted in orthophosphoric acid at 70 °C using a Finnigan-MAT Kiel III carbonate preparation device. Isotopic ratios of purified CO_2 gas were measured on-line with a Finnigan-MAT at the University of Florida and with a Micromass Prism at Santa Cruz. Analytical precision is better than ±0.1 per mil for δ^{18}O in both laboratories. Isotope data from both laboratories were calibrated using the NIST (NBS) 19 standard, and values are reported relative to VPDB (Vienna Pee Dee Belemnite standard).

The age model for site 984 (Fig. 2) was constructed by matching the planktonic and benthic oxygen isotope records to the Ice Volume

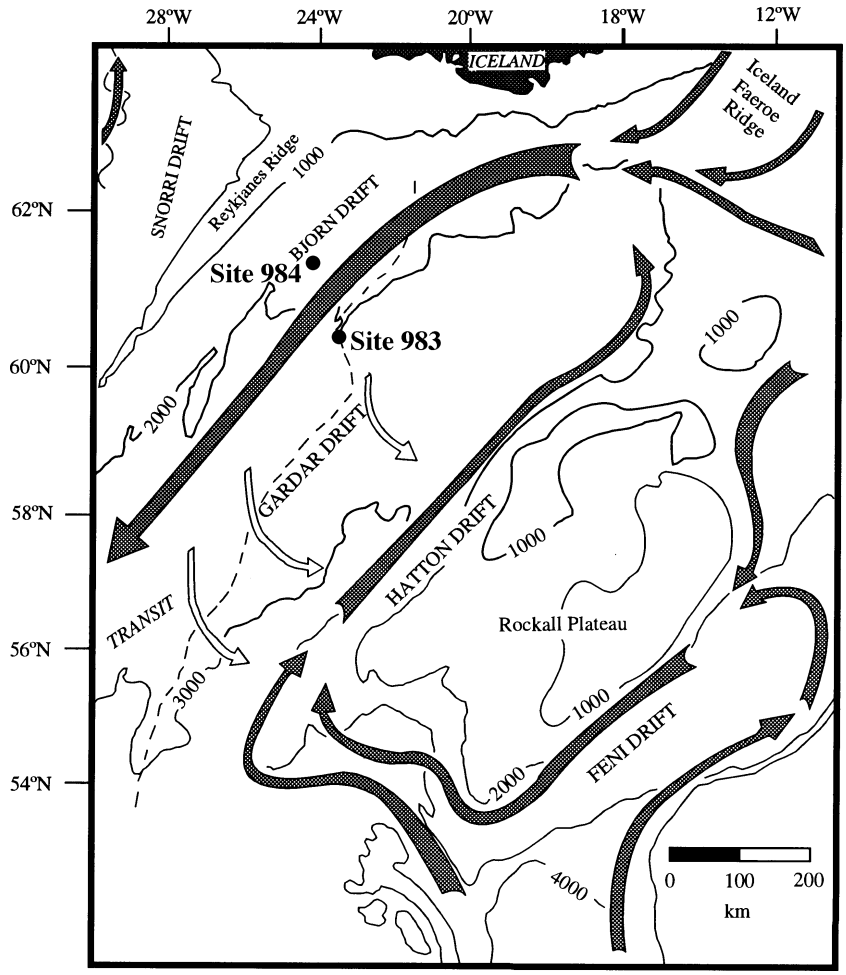

Figure 1. Location map for sites 983 and 984. Bathymetry in metres. The dashed line indicates the crest of the Gardar Drift and the arrows indicate the inferred bottom current flows (map modified from Channell 1999 (see references therein)).

Model of Imbrie & Imbrie (1980) constructed using the 65°N July insolation curve of Berger & Loutre (1991). Linear interpolation between 33 tie-points constitutes the age model. The resulting interval sedimentation rates vary by more than an order of magnitude (3–32 cm kyr^{-1}) (Fig. 3). High sedimentation rates are apparent for glacial marine isotope stages, particularly MIS 20 in the 790–805 ka interval. Sedimentation rates in the 745–790 ka interval spanning the MBB are ∼9 cm kyr^{-1}.

The site 983 age model (Fig. 2) for the 500–700 ka interval (Channell *et al.* 1998) was constructed by matching the δ^{18}O records to those from ODP site 677 (Shackleton *et al.* 1990). The site 983 age model for the 700–900 ka interval (Channell & Kleiven 2000) was constructed by matching the δ^{18}O records to the same Ice Volume Model used here, and then tuning the precession component from the benthic δ^{18}O record to the precession component from the Ice Volume Model. Note that the site 983 age model for the 700–900 ka interval is more detailed (has more tie-points) than that for the 500–700 ka interval (Fig. 3) reflecting the superior resolution of the site 983 δ^{18}O record in the 700–900 ka interval (Fig. 2a).

Support for the site 984 age model is given by the good correlation between the output from a Gaussian filter centred on 20 kyr (0.05 kyr^{-1}) applied to the Ice Volume Model and to the planktonic δ^{18}O record (Fig. 2c). The filter extracts the precession component from both signals, and the satisfactory correlation (Fig. 2c) supports the age model and indicates that the planktonic δ^{18}O record contains a strong ice volume signal. The benthic δ^{18}O has insufficient resolution to yield useful output when the same filter is applied.

4 MAGNETIC PROPERTIES

4.1 Directional data

In conjunction with the determination of the polarity stratigraphy at site 984, stepwise alternating field (AF) demagnetization of 7 cm^3 discrete samples collected from the working half of the composite section indicated that the characteristic magnetization is isolated at peak demagnetization fields above 20 mT (Channell & Lehman 1999). A steep downward-directed magnetization component, interpreted as a secondary magnetization imposed by the drill-string, is lost at peak fields below 20 mT.

During ODP leg 162, archive halves of core sections from site 984 were demagnetized at peak fields up to 25 mT using the shipboard pass-through magnetometer (Channell & Lehman 1999). u-channel samples, collected post-cruise from the archive halves of the site 984 composite section, were stepwise demagnetized in 5 mT steps from

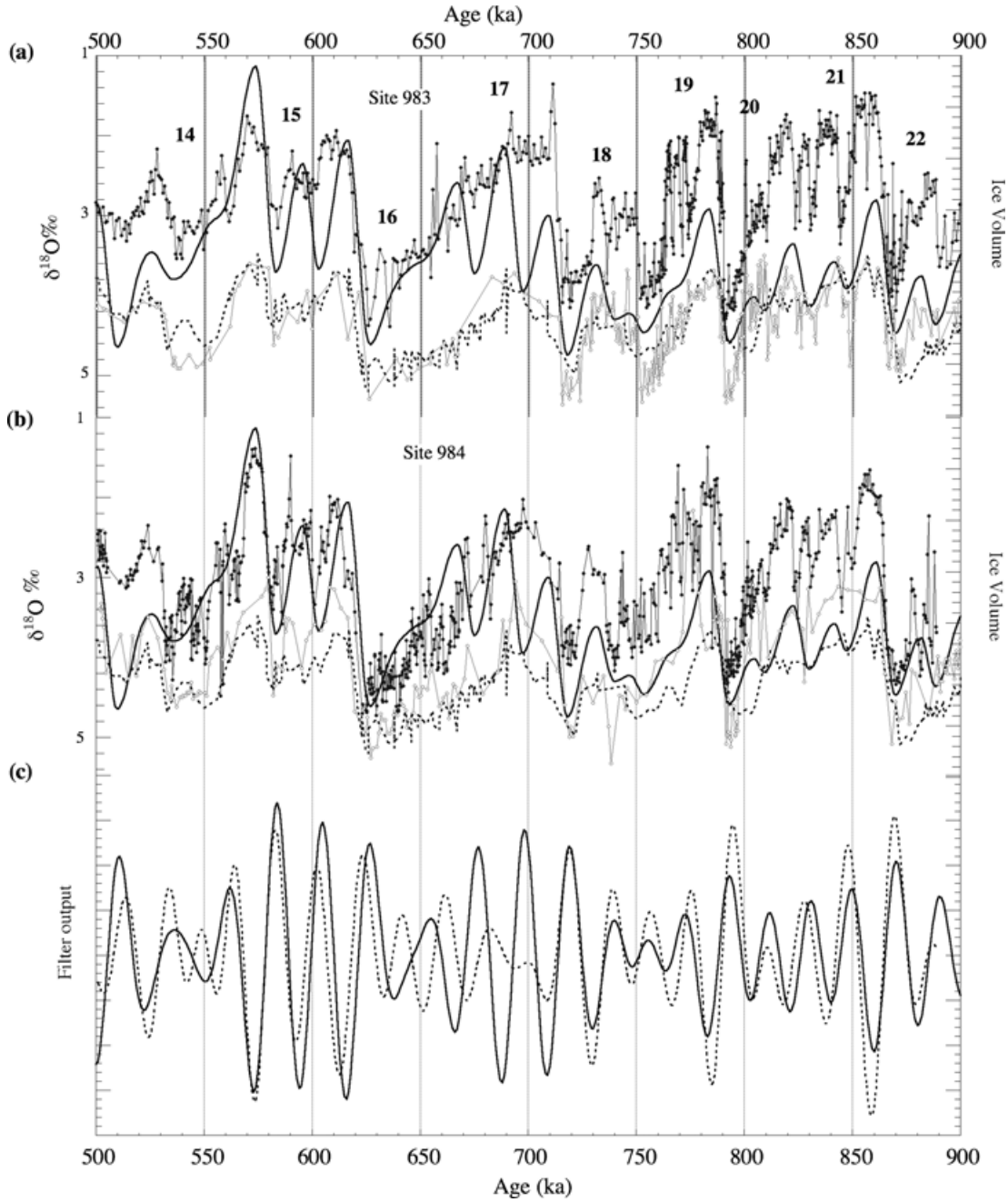

Figure 2. Planktonic (closed symbols, black line) and benthic (open symbols, grey line) δ^{18}O data with the Ice Volume Model (thick black line) and the benthic record from ODP site 677 (dashed line) (Shackleton *et al.* 1990). (a) ODP site 983 data placed on the age models of Channell *et al.* (1998) and Channell & Kleiven (2000). Bold numbers indicate marine isotope stages. (b) ODP site 984 data placed on the age model (this paper) based on correlation of the benthic and planktonic δ^{18}O records to the Ice Volume Model. (c) Output of Gaussian filters centred on 20 kyr (0.05 kyr^{-1}) with a 0.02 kyr^{-1} bandpass applied to the Ice Volume Model (thick line) and planktonic δ^{18}O record (dashed line) for the site 984 age model as in part (b).

peak fields of 15 mT to 60 mT using a 2G-Enterprises u-channel magnetometer. Measurements were made at 1 cm intervals, although each measurement at this spacing is not independent of the next due to the ∼4 cm width of the response function of the magnetometer pick-up coils (Weeks *et al.* 1993; Guyodo *et al.* 2002). Orthogonal projections of u-channel demagnetization data indicate that a magnetization component can be resolved in the 30–60 mT demagnetization interval (Figs 4a and b). The characteristic magnetization component direction, at 1 cm intervals down-core, was then computed for the 30–60 mT demagnetization interval using the standard least-squares method (Kirschvink 1980) (Fig. 5). The maximum angular deviation (MAD) values are generally less than 5° indicating that the component directions are usually well defined. In Fig. 5, the site 984 component magnetization directions are compared with those from site 983 from Channell & Kleiven (2000) for the 700–900 ka interval. For both sites 983 and 984, declinations were 'corrected' using data from the shipboard core-orientation (tensor) tool applied to individual cores. For some cores, tensor data are not available, or are of poor quality, and for these cores the declination correction was performed by rotating individual cores such that

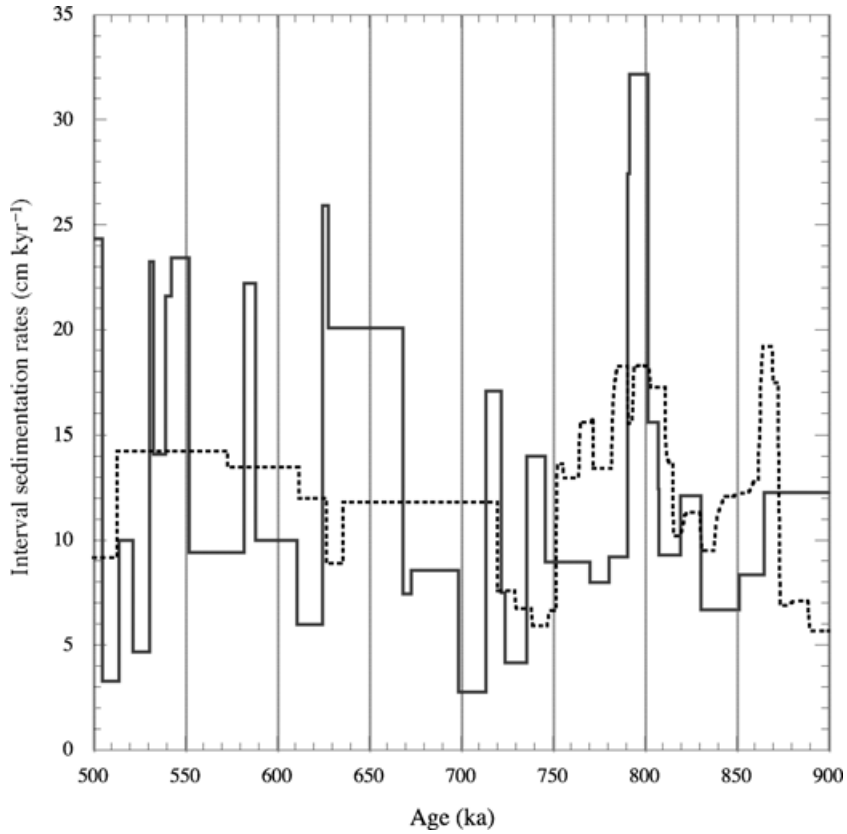

Figure 3. Solid line: interval sedimentation rates for the site 984 age model based on correlation of the benthic and planktonic δ^{18}O records to the Ice Volume Model (this paper). Dashed line: interval sedimentation rate variations for ODP site 983 (Channell *et al.* 1998; Channell & Kleiven 2000).

the *mean* core declination is oriented north (360°) in the Brunhes Chronozone or south (180°) in the Matuyama Chronozone.

4.2 Palaeointensity data

Palaeointensity proxies in sediments have been constructed by dividing (normalizing) the NRM intensity by a magnetic parameter sensitive to changes in the concentration of magnetic grains. The ideal normalizer activates the same grains that carry NRM, thereby compensating for down-core variations in the concentration of remanence-carrying grains. Three bulk magnetic parameters have been used as normalizers to produce palaeointensity proxies: volume susceptibility (κ), anhysteretic remanence (ARM) and isothermal remanence (IRM). Susceptibility is not usually selected as it is sensitive to large multidomain magnetite grains (often a constituent of ice-rafted debris) as well as small (superparamagnetic) grains, neither of which are important carriers of stable magnetic remanence. For samples from site 984, the ARM was acquired in a 100 mT alternating field with a 0.05 mT DC bias field, and the IRM was acquired in a 500 mT DC field. ARM and IRM were AF demagnetized in peak fields of 35 and 45 mT, and measured at 1 cm intervals down-core.

Coercivity spectra, blocking temperature spectra and hysteresis ratios from previous magnetic studies of site 983 (Channell *et al.* 1997, 1998) and of the 0–500 ka interval at site 984 (Channell 1999), indicate that PSD magnetite is the principal remanence carrier at both sites. The plot of anhysteretic susceptibility (κ_{ARM}) against susceptibility (κ) for the 500–900 ka interval at site 984 yields a quasi-linear relationship consistent with fairly uniform magnetite grain size in the 5–10 μm range (Fig. 6). Susceptibility (κ), IRM and ARM intensities vary by less than an order of magnitude in the 500–900 ka interval, and are partly controlled by the percentage of carbonate which varies in the 0–30 per cent range (Fig. 7). The magnetic properties of these sediments appear to lie within the criteria advocated for development of useful palaeointensity proxies (King *et al.* 1983; Tauxe 1993).

The two candidates for the palaeointensity proxy (NRM/ARM and NRM/IRM), calculated for a particular demagnetization step, yield very similar patterns of variability. As for the 0–500 ka interval at site 984 (Channell 1999), NRM/ARM varies with demagnetization step whereas values of NRM/IRM are more or less invariant with demagnetization step. This indicates that the coercivity spectrum of IRM is a good match to the coercivity spectrum of NRM, and is therefore more likely (than ARM) to activate the grains that carry NRM. Here we use the arithmetic mean of NRM/IRM after demagnetization at 35 mT and 45 mT as the palaeointensity proxy. NRM/IRM was also used as the palaeointensity proxy for site 983 (Channell *et al.* 1998; Channell & Kleiven 2000).

Prominent lows in the palaeointensity proxies for sites 983 and 984 correspond to low values of virtual geomagnetic polar (VGP) latitude. The more prominent VGP excursions, to values $<20°$, have estimated ages of 540 ka, 590 ka and 670 ka (Figs 8a and b). These apparent geomagnetic excursions can be tentatively correlated to excursions recognized elsewhere (Table 1). Candidates for correlative excursions include the Big Lost excursion with an estimated age of 565 ka (Champion *et al.* 1988) and the 'La Palma' excursion at ~602 ka (Quidelleur *et al.* 1999). Both these

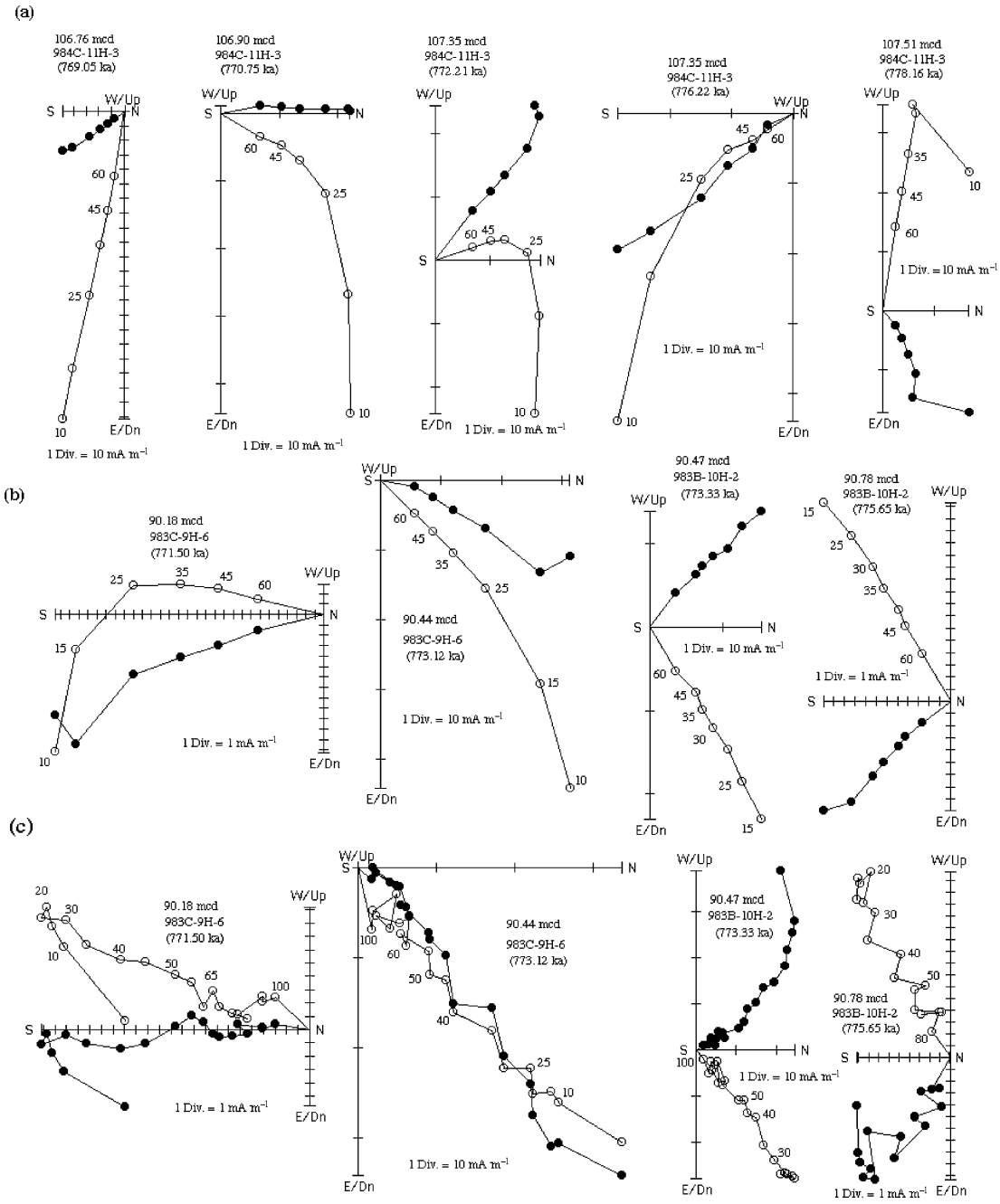

Figure 4. Orthogonal projection of alternating field demagnetization data for u-channel samples across the Matuyama–Brunhes boundary from (a) hole 984C, (b) holes 983C and 983B, and (c) for 1 cm discrete samples from the same site 983 intervals as in (b). Open and closed symbols indicate projection on the vertical and horizontal planes respectively. The estimated ages and stratigraphic positions of the sample in metres composite depth (mcd) are indicated.

excursions have been recognized in volcanic rocks in Idaho and in the Canary Islands respectively, and dated using K/Ar methods. The 'Delta' palaeointensity low, first labelled as such in the ODP leg 138 palaeointensity record (Valet & Meynadier 1993) at about 690 ka, appears to be associated with a thin but well-defined reverse polarity subzone in the 1.7 km drill-core from Osaka Bay (Biswas *et al.* 1999). An age of 690 ka for this polarity subzone was based on age interpolation between the MBB and an ash layer dated at 24 ka. Directional excursions recorded in sediments from ODP leg 172 (Lund *et al.* 2001) and from ODP site 980 (Channell & Raymo 2003) have been correlated to MIS 17, and have similar estimated ages (∼690 ka).

Other published palaeointensity records from sites with mean sedimentation rates varying from 0.69 cm kyr^{-1} to 3 cm kyr^{-1} (Fig. 8c) indicate two broad palaeointensity highs at 630–670 ka and 720–770 ka separated by the intervening (Delta) palaeointensity low. Many of the higher-frequency features in the site 983 and 984 palaeointensity records (Fig. 8b) are not seen in the other records (Fig. 8c), presumably due to their low sedimentation rates (0.69–3 cm kyr^{-1}). For the records shown in Fig. 8(c), age control was based on a variety of sources. For the California margin record (ODP site 1021), it was based on a correlation of the susceptibility record to a reference δ^{18}O curve (Guyodo *et al.* 1999). The age control for the leg 138 record (Valet & Meynadier 1993) was based on orbital

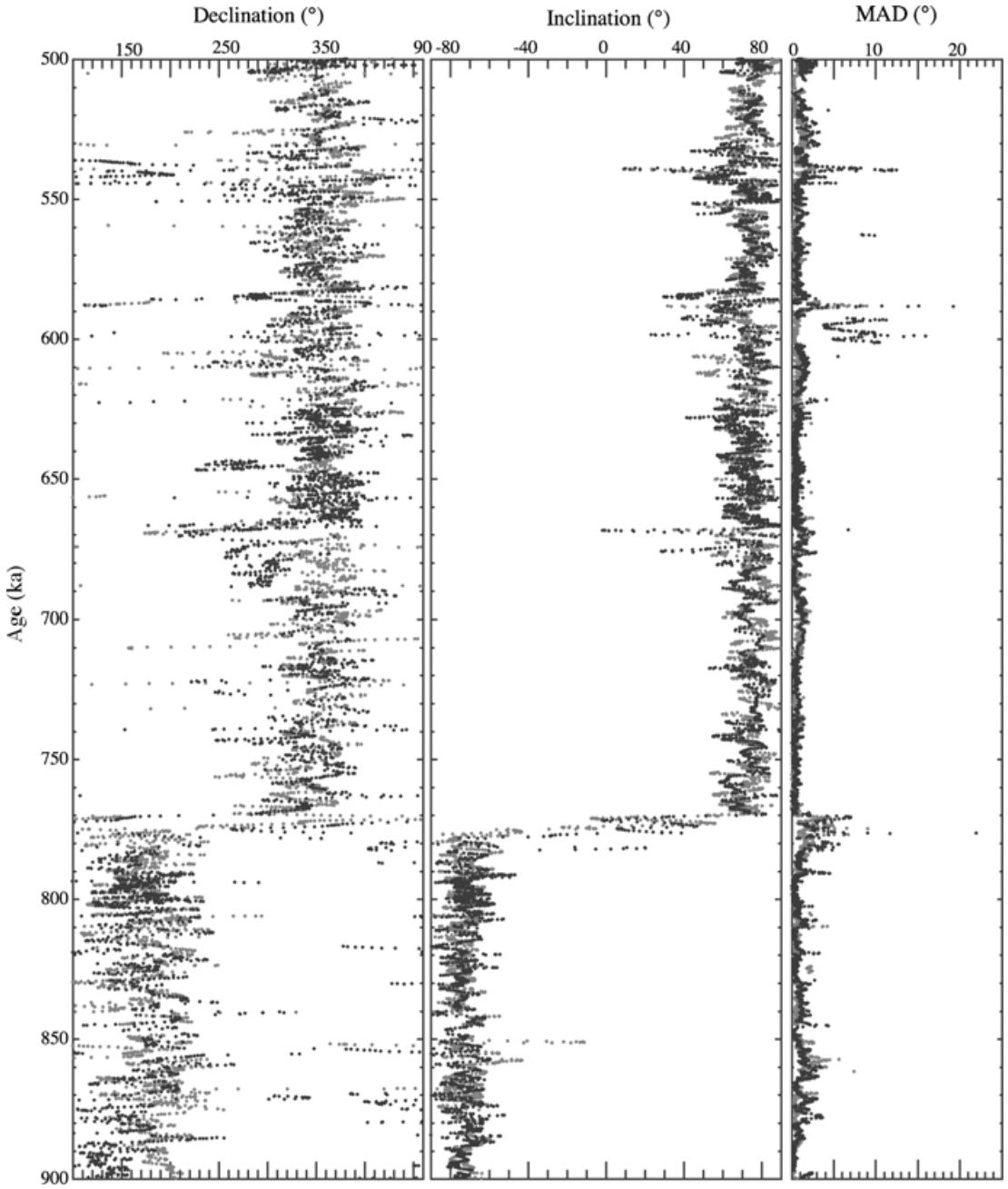

Figure 5. Component declinations and inclinations for sites 983 (open grey symbols) and 984 (closed black symbols), and corresponding maximum angular deviation (MAD) values, computed at 1 cm intervals down-core for the 30–60 mT demagnetization interval using the standard 3-D least-squares method (Kirschvink 1980).

tuning of the GRAPE density stratigraphy (Shackleton *et al.* 1995). The chronology for the Indian Ocean record (Meynadier *et al.* 1994) was based on susceptibility correlation to a nearby site (ODP site 709). The Sint-800 composite stack (Guyodo & Valet 1999), the dashed line in Fig. 8(c), was compiled from 10 records for the 500–800 ka interval, including ODP site 983 and all the records shown in Fig. 8(c) apart from the Pacific record of Yamazaki (1999). The age control for this Pacific record was produced by matching the *S* ratio (a magnetic parameter sensitive to eolian dust) to a reference δ^{18}O curve.

The issue of orbital modulation of geomagnetic palaeointensity has been a subject of recent controversy, as orbital power has shown up in a number of Atlantic and Pacific palaeointensity records (Channell & Lehman 1997; Yamazaki 1999; Guyodo *et al.* 2000; Yamazaki & Oda 2002; Roberts *et al.* 2003). As for the 0–500 ka interval at site 984 (see Channell *et al.* 1998; Channell 1999), the palaeointensity record in the 500–900 ka interval at this site has significant power at periods of 100 kyr (Fig. 9). Coherent 100 kyr power is also present in the normalizer (IRM) used to obtain the palaeointensity proxy (Fig. 9). This implies that the 100 kyr power in both the concentration parameter (IRM) and the palaeointensity proxy were derived from climatically driven lithological variations. Based on wavelet analysis and numerical modelling of the 0–1.2 Ma palaeointensity record from site 983, Guyodo *et al.* (2000) concluded that

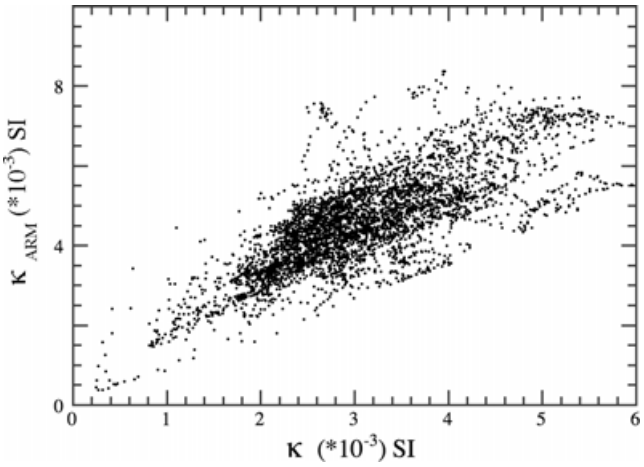

Figure 6. Site 984: anhysteretic susceptibility (κ_{ARM}) plotted against volume susceptibility (κ) for the 500–900 ka (75–123 mcd) interval.

lithological contamination accounts for the orbital power in palaeointensity at site 983 but, fortunately, does not substantially modify the basic shape of the record. The imperfect match between the site 984 and 983 palaeointensity records in Fig. 8(b) may be attributed to lithological/climatic contamination of the palaeointensity records and inadequate age models.

5 MATUYAMA–BRUNHES BOUNDARY (MBB)

For three core sections spanning the MBB at ODP site 983 (sections 983B-10H-1, 983B-10H-2 and 983C-9H-6), 1 cm^3 cube-shaped discrete samples were collected back-to-back alongside the u-channel trough. A total of 388 discrete samples were collected from both the working and archive halves of these three core sections from site 983. From a single archive core section (984A-11H-5) spanning the MBB at site 984, 114 discrete samples were collected, again, back-to-back alongside the u-channel trough.

The discrete sampling was carried out in order to compare 1 cm discrete sample data with u-channel data from the same core sections over the critical MBB interval. Discrete samples were progressively AF demagnetized in 19 steps in the 10–100 mT peak field range. Component magnetization directions were computed using the standard least-squares method (Kirschvink 1980). MAD values are below 15° for all magnetization components derived from the discrete samples, and no samples were excluded.

Orthogonal projections of AF demagnetization data from u-channel samples across the MBB at sites 984 (Fig. 4a) and 983 (Fig. 4b), and for discrete samples from site 983 (Fig. 4c), indicate that the characteristic magnetization component is well resolved in the 30–60 mT demagnetization interval. Interestingly, the discrete samples, collected 6–7 yr after the u-channel samples, do not display any additional 'storage-related' remanence overprint. At site 984, u-channel MAD values computed for the 30–60 mT demagnetization interval are below 10° in the polarity transition zone (Fig. 5). For 1 cm discrete samples, MAD values are always $<15°$ and generally $<10°$.

The MBB is recorded at three holes at site 983 (holes 983A, 983B and 983C) and three holes at site 984 (holes 984A, 984B and 984C). Multiple u-channel records of the characteristic magnetization components across the MBB from different holes, and from archive and working halves at the same hole, combined with the data of Channell & Lehman (1997), allow the reproducibility of the transition record to be tested (Figs 10 and 11). Note that the depths (mcd) derived from the shipboard construction of the composite section may have resulted in imperfect correlation among the holes at a site. In addition, the declination 'correction' for any individual hole may be imperfect. With these caveats in mind, the directional data are reproducible from working halves to archive halves, and many features are reproduced from hole to hole (Figs 10 and 11). The pre-reversal interval of positive inclination in the 107.7–107.9 mcd interval is reproduced at all holes at site 984 but not at site 983.

Using standard Fisher (1953) statistics, mean directions are determined from the three to five u-channel records available at sites 983 (Fig. 10b) and 984 (Fig. 11b). From the mean directions across the MBB, the VGP paths for sites 984 and 983 reproduce a loop over the Pacific followed by a loop over Africa (Fig. 12a). Loop 1 over southeast Asia for site 984 (equivalent to the pre-reversal interval of low/positive inclination in the 107.8–107.9 mcd interval in Fig. 11) is not observed at site 983.

The 1 cm discrete samples from sites 983 and 984 are compared with the u-channel data from the same core sections in Figs 10(c) and (d) and 11(c). As concluded by Guyodo *et al.* (2002) on the basis of comparison of u-channel and discrete samples from ODP site 1090, the u-channel data from site 983 are smoothed with respect to the data from 1 cm discrete samples. Some of the discrete sample 'scatter' may be due to sediment deformation associated with sampling and/or errors associated with the orientation and handling of the 1 cm discrete samples. Nonetheless, the comparison of discrete sample and u-channel data indicates that the u-channel measurement procedure did not introduced spurious artefacts into the polarity transition records, as has been claimed by some authors (e.g. Yang *et al.* 2001).

Comparison of the VGP distribution from discrete samples (Figs 12b–d) with the VGPs computed from the Fisher mean of u-channel data from the same sites (Fig. 12a) indicates three 'clusters' of VGPs in northeast Asia, the South Atlantic and in the Central Pacific. VGP maps derived from u-channel component magnetizations from individual holes at sites 983 and 984 (Channell & Lehman 1997), rather than from the Fisher mean at the site, also reveal these three VGP 'clusters' (Fig. 13).

The MBB occurs between marine isotope substage 19.3 (negative peak associated with MIS 19) and substage 18.4 (oldest positive interval within MIS 18), following the isotopic stage nomenclature of Bassinot *et al.* (1994) (Fig. 14). Tauxe *et al.* (1996) estimated the age of the MBB by adopting ages for substages 18.2, 18.4 and 20.2 of 717 ka, 753 ka and 792 ka respectively, and assuming constant sedimentation rates between identifiable substages in 18 deep-sea cores. Using the same approach, we estimate an age of 774.6 ka for the mid-point of the MBB at site 984. Our site 984 age model, based on fit of the isotope data to the Ice Volume Model, yields an age of 773.5 ka for the mid-point of the MBB (Fig. 14).

6 CONCLUSIONS

ODP sites 984 and 983 provide high-resolution (high-sedimentation-rate) oxygen isotope and magnetic records across the MBB. The age model for site 984 is based on the correlation of the oxygen isotope record to the Ice Volume Model (Imbrie & Imbrie 1980) computed using a more recent 65°N July insolation curve (Berger & Loutre 1991). The site 984 age model results in satisfactory match of the precessional components from the Ice

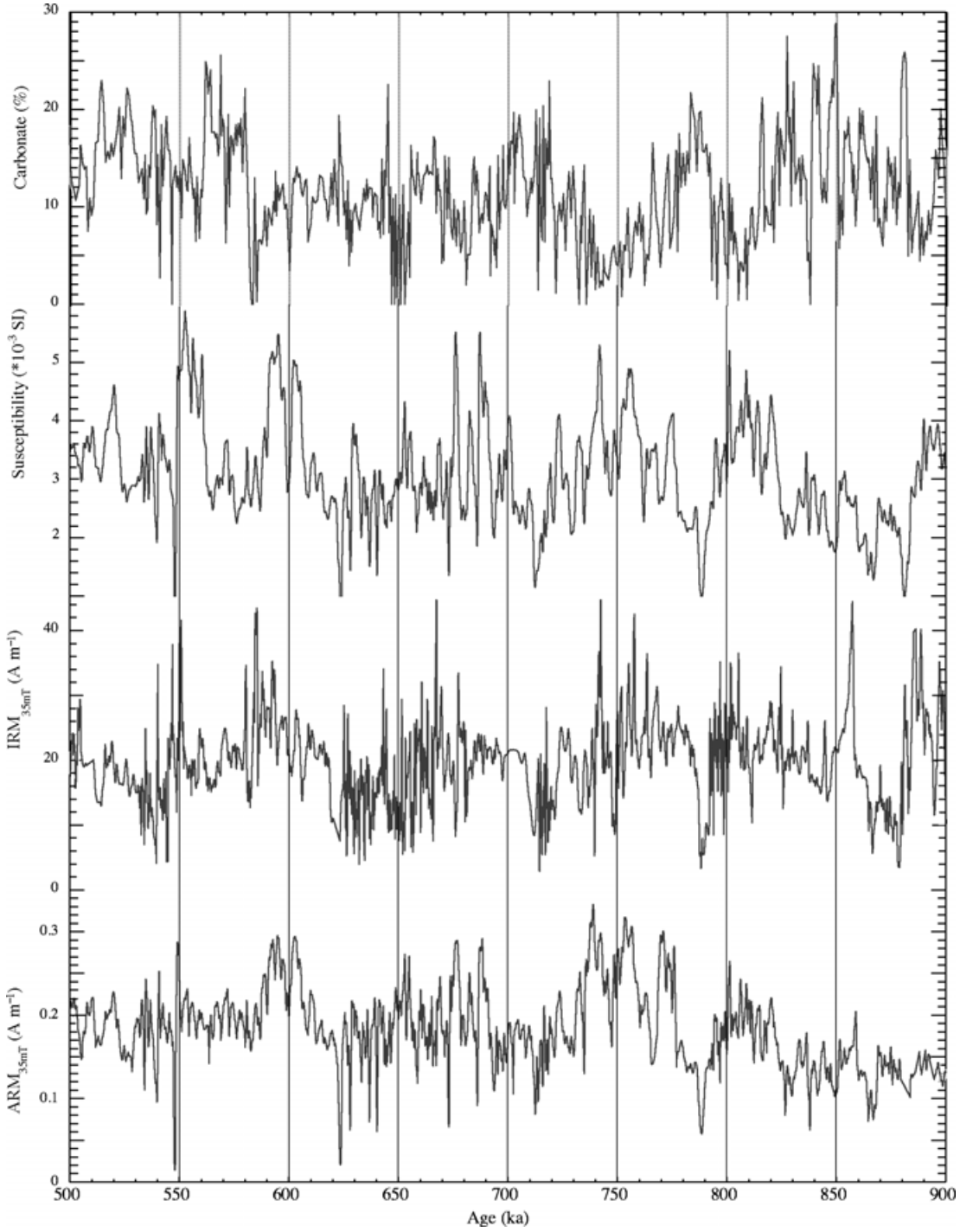

Figure 7. Site 984: carbonate percentage, u-channel volume susceptibility, IRM and ARM intensities after demagnetization at peak fields of 35 mT. Carbonate data from Ortiz *et al.* (1999).

Volume Model and the planktonic δ^{18}O record (Fig. 2). Using this isotope-based age model, the palaeointensity record from site 984 can be satisfactorily matched to that from site 983 (Fig. 8b). Palaeointensity lows correspond to lows in VGP latitude at both sites (Fig. 8), implying that palaeointensity lows are accompanied by directional excursions, or possibly imperfectly recorded brief polarity subchrons, at 540, 590 and 670 ka.

At site 984, the Matuyama–Brunhes polarity transition, as defined by virtual geomagnetic polar (VGP) latitudes $<50^{\circ}$, has an apparent duration of 7 kyr with an *onset* at 777 ka and a mid-point at ∼773.5 ka. At site 983, the mid-point of the transition was found to be at 772.5 ka and the apparent duration of the transition was about 5 kyr (Channell & Kleiven 2000). In the vicinity of the MBB, the palaeointensity records for sites 983/984 (Fig. 8b) show a low at 790 ka followed by a recovery prior to a prolonged palaeointensity low (782–770 ka) at the MBB. The palaeointensity low at about 790 ka pre-dates the directional change at the Matuyama–Brunhes boundary (Fig. 8).

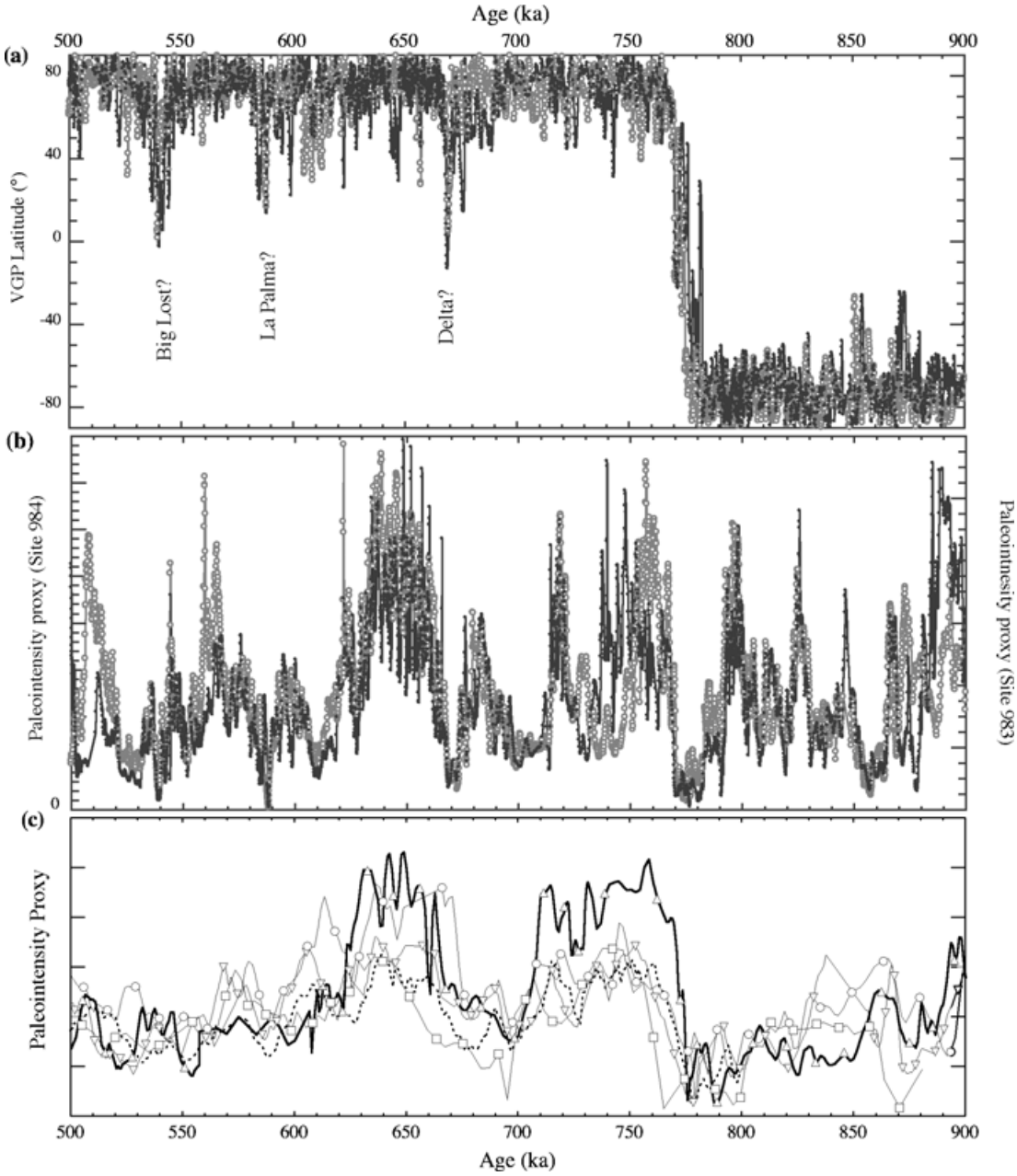

Figure 8. (a) Virtual geomagnetic polar (VGP) latitudes for sites 984 (closed black symbols) and 983 (open grey symbols). (b) Palaeointensity proxies for sites 984 (closed black symbols) and 983 (open grey symbols). (c) Other palaeointensity records for the 500–900 ka interval placed on their published age models. Mean sedimentation rates for the Brunhes Chron are given in brackets after each reference: triangles, equatorial Pacific ODP leg 138 (Valet & Meynadier 1993) (1.8 cm kyr^{-1}); inverted triangles, California Margin ODP site 1021 (Guyodo & Valet 1999) (3.7 cm kyr^{-1}); circles, Indian Ocean core MD90-0940 (Meynadier *et al.* 1994) (1.3 cm kyr^{-1}); squares, north-central Pacific core NGC-69 (Yamazaki 1999) (0.69 cm kyr^{-1}); dashed line, Sint-800 composite stack (Guyodo & Valet 1999).

Table 1. Directional excursions (and palaeointensity lows) in the 500–900 ka interval at sites 983/984.

Label: derived from correlative occurrences	Estimated age at sites 983/984 (ka)	Marine isotope stage at sites 983/984	Ref. for correlative occurrences
Big Lost	540	14	Champion *et al.* (1988)
La Palma	590	15	Quidelleur *et al.* (1999)
Delta	670	17	Biswas *et al.* (1999), Lund *et al.* (2001), Channell & Raymo (2003)

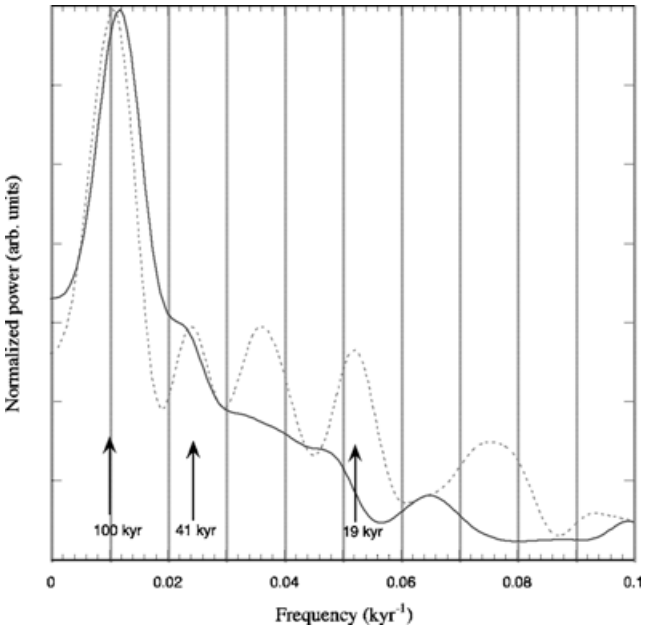

Figure 9. Power spectra for the palaeointensity proxy (mean NRM/IRM) (solid line) and for $IRM_{35\,mT}$ (dashed line) derived using the Blackman–Tukey method and AnalySeries software (Paillard *et al.* 1996).

The mid-points of the Matuyama–Brunhes polarity transition at sites 984 and 983 are both younger than the weighted mean ages of 778.7 ± 1.9 ka based on a 1996 review of MBB $^{40}Ar/^{39}Ar$ ages (Singer & Pringle 1996). A more recent review of the age of the MBB, including a large number of new ages for the Bishop Tuff, yield an age for the polarity reversal of 774.2 ± 2.8 ka (Sarna-Wojcicki *et al.* 2000). As pointed out by these authors, however, the 2.7 per cent range of generally accepted ages used for $^{40}Ar/^{39}Ar$ standards severely limits the ability of the $^{40}Ar/^{39}Ar$ method to improve our estimate of the MBB age. Tauxe *et al.* (1996) gave an MBB age of 777.9 ka (±1.8) based the position of the MBB within MIS 19 at 18 deep-sea sites, and an age of 778.0 ka (±1.7) based on a combination of this MIS 19 estimate with the available $^{40}Ar/^{39}Ar$ ages. The apparent age for the mid-point of the MBB reversal from sites 983 and 984 (Fig. 14) is younger than these estimates, and younger than the generally adopted astrochronological estimate (780 ka) (Shackleton *et al.* 1990). A possible explanation for this 4–5 kyr discrepancy is that the effective lock-in depth for remanence acquisition has greater temporal significance at sites with a lower sedimentation rate (from which the astrochronological estimates have been derived) than at sites with a higher sedimentation rate such as 983 and 984 (see Channell & Guyodo 2004).

Volcanic sequences that record the MBB palaeointensity low often fail to capture transitional magnetization directions due, presumably, to the sporadic nature of volcanic eruption and the low probability of capturing brief geological events such as polarity transitions. VGP clusters rather than VGP paths characterize the volcanic records of the MBB transition, and these clusters tend to be located in the region of Australia or off South America (Hoffman 1992). The location of the transitional VGP cluster appears to be broadly dependent on site location, indicating that transitional fields were not dipolar (Hoffman & Singer 2004). The similarity in location of VGP clusters from one reversal to another, both in volcanic (Hoffman & Singer 2004) and sedimentary data (e.g. Channell & Lehman 1997; Mazaud & Channell 1999, this paper), indicates that transitional field configurations persisted on million-year time scales. The South American and Australian VGP clusters, and to a lesser extent the northeast Asian cluster, can be matched to the vertical flux patches in the modern NAD field at the Earth's surface, to flux patches in the modern field at the surface of the core and to fast seismic wave velocities in the lower mantle (see Hoffman 1992; Hoffman & Singer 2004).

At sites 984 and 983, well-defined magnetization components can be tracked across the MBB polarity transition. The component directions are reproducible from working to archive halves of core sections, for both u-channel and 1 cm discrete samples, between holes within a site and between sites (Figs 10 and 11). As a result, VGP paths for the MBB from sites 983 and 984 are sufficiently similar from hole to hole, and from u-channels to discrete samples, that artefacts due to the u-channel measurement procedure cannot provide an adequate explanation for the complexity of the paths (Figs 12 and 13). The discrete sample data from sites 983 and 984 indicate that VGPs at the MBB jump abruptly from one VGP cluster to another and that u-channel VGP paths between clusters are largely a result of the smoothing inherent in u-channel data. The South Atlantic and northeast Asian VGP clusters account for the observation that lower-sedimentation-rate VGP records for the MBB often lie along American or east Asian longitudes.

ACKNOWLEDGMENTS

Research supported by US National Science Foundation (EAR-98-04711). We are indebted to the staff of the Ocean Drilling Program (ODP), particularly the staff at the Bremen core repository, and our ODP leg 162 colleagues for facilitating this study. Brad Clement and Alain Mazaud provided constructive reviews of an earlier version of the manuscript.

REFERENCES

Bassinot, F., Labeyrie, L., Vincent, E., Quidelleur, X., Shackleton, N. & Lancelot, Y., 1994. The astronomical theory of climate and the age of the Brunhes-Matuyama magnetic reversal, *Earth planet. Sci. Lett.,* **126,** 91–108.

Berger, A. & Loutre, M.F., 1991. Insolation values for the climate of the last 10 million years, *Q. Sci. Rev.,* **10,** 297–317.

Biswas, D.K., Hyodo, M., Taniguchi, Y., Kaneko, M., Katoh, S., Sato, H., Kinugasa, Y. & Mizuno, K., 1999. Magnetostratigraphy of Plio-Pleistocene sediments in a 1700-m core from Osaka Bay, southwestern Japan and short geomagnetic events in the middle Matuyama and early Brunhes chrons, *Palaeogeog. Palaeoclimatol. Palaeoecol.,* **148,** 233–248.

Champion, D.E., Lanphere, M.A. & Kuntz, M.A., 1988. Evidence for a new geomagnetic reversal from lava flows in Idaho: discussion of short polarity reversals in the Brunhes and late Matuyama polarity chrons, *J. geophys. Res.,* **93,** 11 667–11 680.

Channell, J.E.T., 1999. Geomagnetic paleointensity and directional secular variation at Ocean Drilling Program (ODP) Site 984 (Bjorn Drift) since 500 ka: comparisons with ODP Site 983 (Gardar Drift), *J. geophys. Res.,* **104,** 22 937–22 951.

Channell, J.E.T. & Guyodo, Y., 2004. The Matuyama Chronozone at ODP Site 982 (Rockall Bank): evidence for decimeter-scale magnetization lock-in depths, in *Timescales of the Paleomagnetic Field,* AGU Geophysical Monograph, eds Channell, J.E.T., Kent, D.V., Lowrie, W. & Meert, J., American Geophysical Union, Washington, DC, in press.

Channell, J.E.T. & Kleiven, H.F., 2000. Geomagnetic palaeointensities and astrochronological ages for the Matuyama-Brunhes boundary and the boundaries of the Jaramillo Subchron: palaeomagnetic and oxygen isotope records from ODP Site 983, *Phil. Trans. R. Soc. Lond.,* A, **358,** 1027–1047.

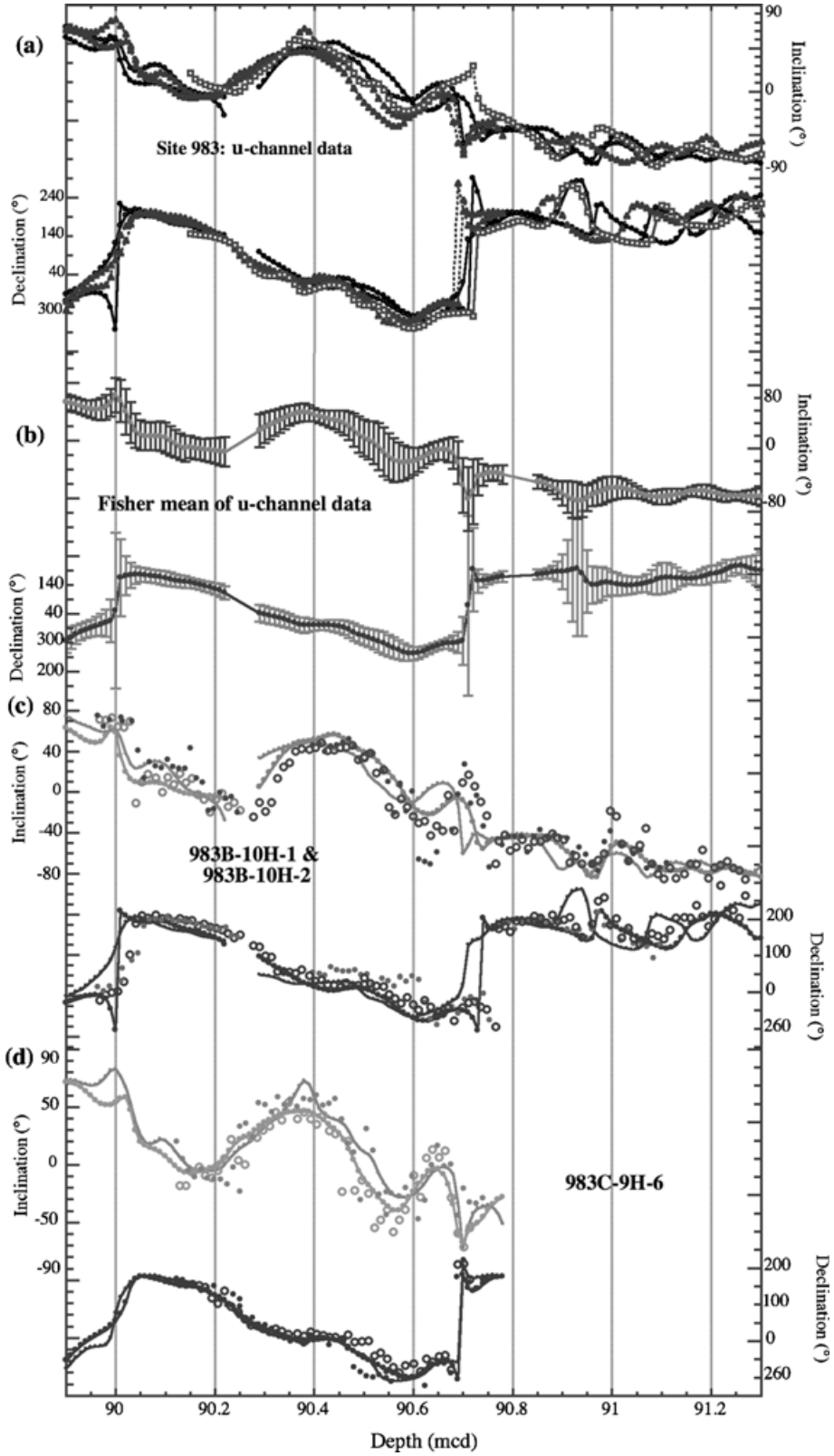

Figure 10. Site 983. (a) Component declinations and inclinations computed for the 30–60 mT peak field demagnetization interval from u-channel samples: hole 983A, working half (open squares); hole 983B, archive half (closed circles), working half (open circles); hole 983C, archive half (closed triangles), working half (open triangles). (b) Mean directions calculated each 1 cm for three to five individual u-channel records using standard Fisher (1953) statistics. Error bars have a half-length of α_{95} for inclination and $\alpha_{95}/\cos I$ for declination. (c) u-channel data for core sections 983B-10H-1 and 983B-10H-2 from working (closed symbols joined by line) and archive halves (open symbols joined by line), and for 1 cm discrete samples from working (closed symbols, no line) and archive halves (open symbols, no line). (d) Data from core section 983C-9H-6 (same notation as for (c)).

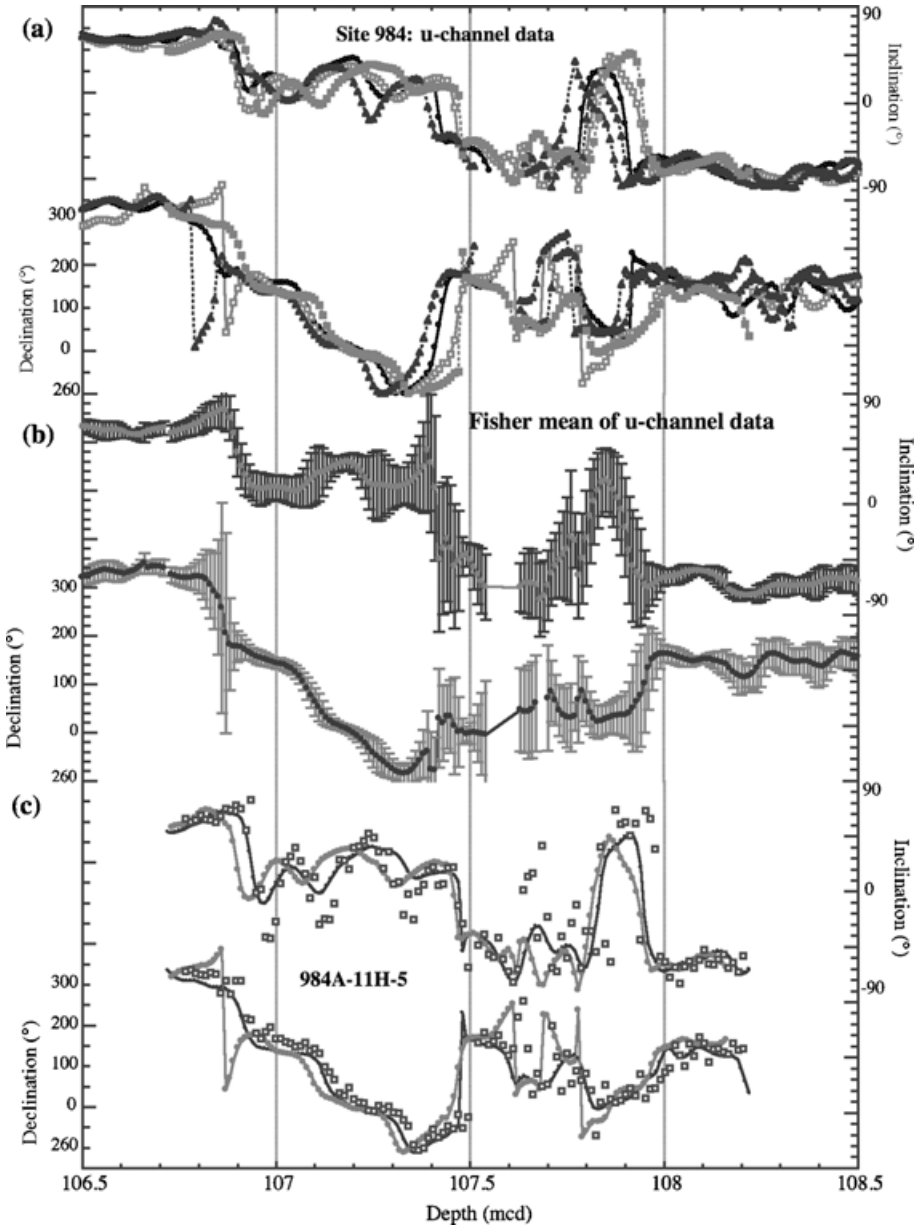

Figure 11. Site 984. (a) Component declinations and inclinations computed for the 30–60 mT peak field demagnetization interval from u-channel samples: hole 984A, archive half (closed squares, dashed line), working half (open squares, dashed line); hole 984B, working half (open circles, continuous line); hole 984C, archive half (closed triangles, dashed line) and working half (open triangles, dashed line). (b) Mean directions calculated each 1 cm for three to five individual u-channel records using standard Fisher (1953) statistics. Error bars have a half-length of α_{95} for inclination and $\alpha_{95}/\cos I$ for declination. (c) u-channel data for core sections 984A-11H-5 from working (closed symbols joined by line) and archive halves (open symbols joined by line), and for 1 cm discrete samples from archive halves (open symbols, no line).

Channell, J.E.T. & Lehman, B., 1997. The last two geomagnetic polarity reversals recorded in high-deposition-rate sediment drifts, *Nature,* **389,** 712–715.

Channell, J.E.T. & Lehman, B., 1999. Magnetic stratigraphy of Leg 162 North Atlantic Sites 980–984, in *Proc. ODP, Sci. Results,* **162**, pp. 113–130, eds Jansen, E., Raymo, M.E., Blum, P. & Herbert, T., Ocean Drilling Program, College Station, TX.

Channell, J.E.T. & Raymo, M.E., 2003. Paleomagnetic record at ODP Site 980 (Feni Drift, Rockall) for the past 1.2 Myrs, *Geochem. Geophys. Geosyst.,* doi:10.1029/2002GC000440.

Channell, J.E.T., Hodell, D.A. & Lehman, B., 1997. Relative geomagnetic paleointnesity and δ^{18}O at ODP Site 983 (Gardar Drift, North Atlantic) since 350 ka, *Earth planet. Sci. Lett.,* **153,** 103–118.

Channell, J.E.T., Hodell, D.A., McManus, J. & Lehman, B., 1998. Orbital modulation of geomagnetic paleointensity, *Nature,* **394,** 464–468.

Channell, J.E.T., Mazaud, A., Sullivan, P., Turner, S. & Raymo, M.E., 2002. Geomagnetic excursions and paleointensities in the 0.9-2.15 MA interval of the Matuyama Chron at ODP Site 983 and 984 (Iceland Basin). *J. Geophys. Res.,* **107 (B6),** 10.1029/2001JB000491.

Channell, J.E.T., Labs, J. & Raymo, M.E., 2003. The Réunion Subchronozone at ODP Site 981 (Feni Drift, North Atlantic), *Earth planet. Sci. Lett.,* **215,** 1–12.

Clement, B.M., 1991. Geographical distribution of transitional VGPs: evidence for non-zonal equatorial symmetry during the Matuyama–Brunhes geomagnetic reversal, *Earth planet. Sci. Lett.,* **104,** 48–58.

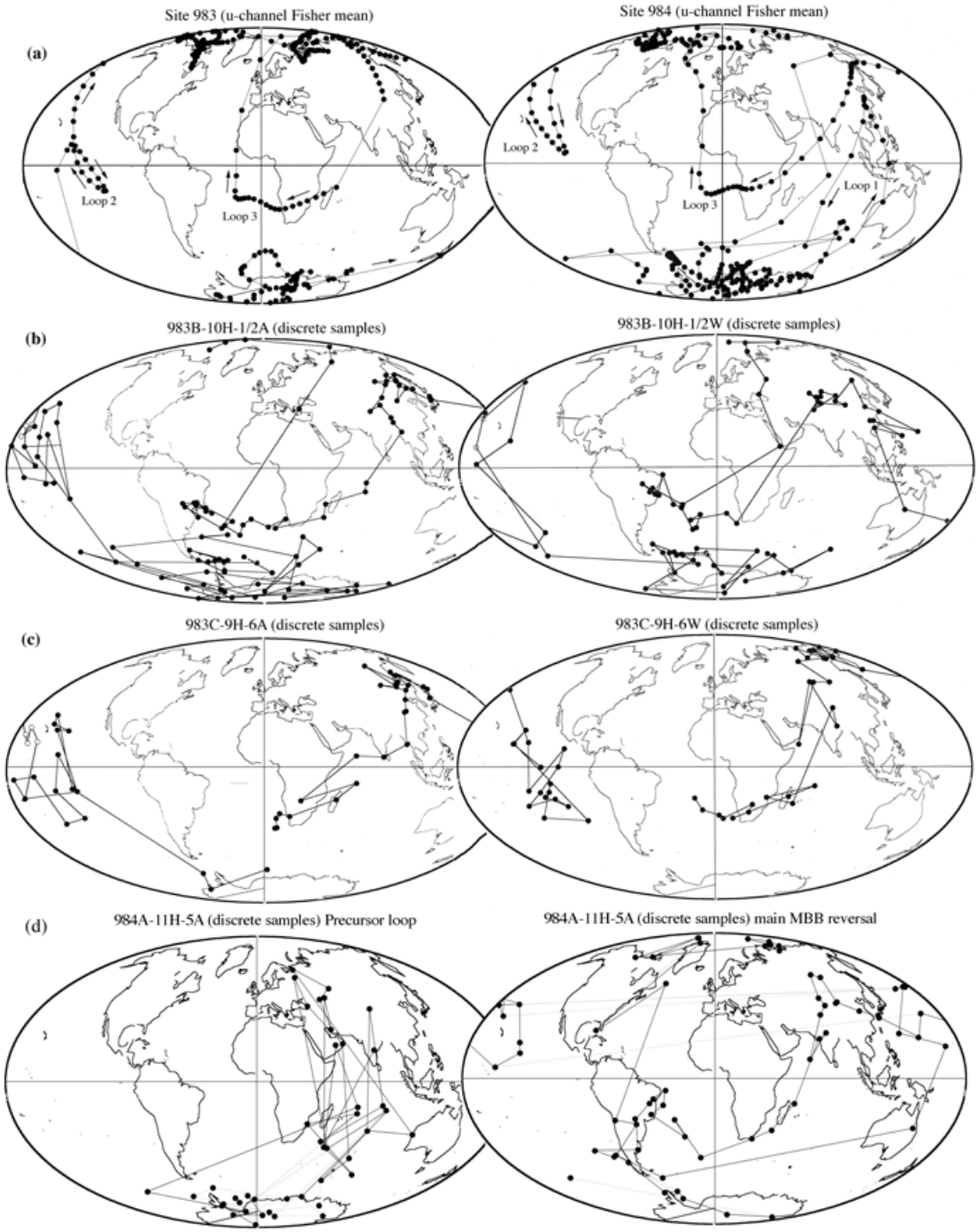

Figure 12. (a) Virtual geomagnetic poles (VGPs) for the Matuyama–Brunhes boundary (MBB) interval calculated from sites 983 and 984 u-channel mean directions (from Figs 10b and 11b). Loop 1 (pre-reversal) is observed at site 984, but not at site 983. Arrows and loop numbers indicate time progression. (b) VGPs for 1 cm discrete samples collected from archive (A) and working halves (W) from core sections 983B-10H-1 and 983B-10H-2. (c) VGPs for 1 cm discrete samples collected from archive (A) and working halves (W) from core section 983C-9H-6. (d) VGPs for 1 cm discrete samples collected from archive half of core section 984A-11H-5 for pre-reversal loop 1 (left) in the 107.62–108.20 mcd interval, and for the MBB transition (right) in the 106.77–107.62 mcd interval.

Clement, B.M. & Kent, D.V., 1987. Geomagnetic polarity transition records from five hydraulic piston core sites in the North Atlantic, in *Initial Reports, DSDP 94,* pp. 831–852, eds Ruddimann, W.F., Kidd, R.B., Thomas, E. *et al.,* US Government Printing Office, Washington, DC.

Clement, B.M. & Kent, D.V., 1991. A southern hemisphere record of the Matuyama–Brunhes polarity reversal, *Geophys. Res. Lett.,* **18,** 81–84.

Dziewonski, A.M., 1984. Mapping the lower mantle: determination of lateral heterogeneity in P velocity up to degree and order 6, *J. geophys. Res.,* **89,** 5929–5952.

Fisher, R.A., 1953. Dispersion on a sphere, *Proc. R. astr. Soc.,* **A217,** 295–305.

Flower, B.P., Oppo, D.W., McManus, J.F., Venz, K.A., Hodell, D.A. & Cullen, J.A., 2000. North Atlantic intermediate to deep water circulation and

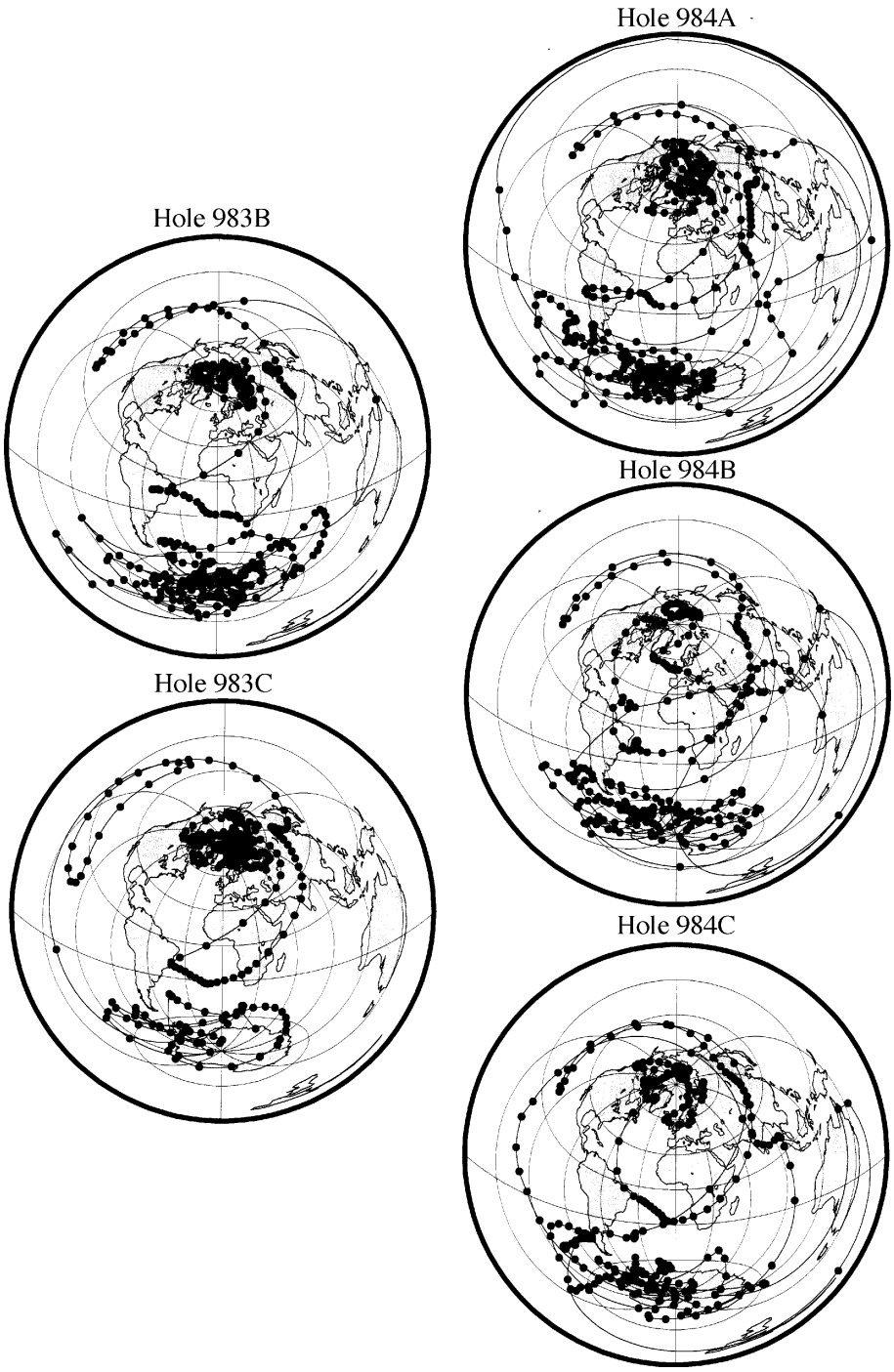

Figure 13. Virtual geomagnetic poles (VGPs) for the Matuyama–Brunhes boundary (MBB) interval derived from u-channel data from individual holes at sites 983 and 984 (redrawn from Channell & Lehman 1997).

chemical stratification during the past 1 Myr, *Paleoceanography,* **15,** 388–403.

Guyodo, Y. & Channell, J.E.T., 2002. Effects of variable sedimentation rates and age errors on the resolution of sedimentary paleointensity records, *Geochem. Geophys. Geosyst.,* doi:10.1029/2001GC000211.

Guyodo, Y. & Valet, J.-P., 1999. Global changes in intensity of the earth's magnetic field during the past 800 kyr, *Nature,* **399,** 249–252.

Guyodo, Y., Richter, C. & Valet, J.-P., 1999. Paleointensity record from Pleistocene sediments (1.4-0 Ma) off the California Margin, *J. geophys, Res.,* **104,** 22 953–22 964.

Guyodo, Y., Gaillot, P. & Channell, J.E.T., 2000. Wavelet analysis of relative geomagnetic paleointensity at ODP Site 983, *Earth planet. Sci. Lett.,* **184,** 109–123.

Guyodo, Y., Channell, J.E.T. & Thomas, R., 2002. Deconvolution of u-channel paleomagnetic data near geomagnetic reversals and short events, *Geophys. Res. Lett.,* **29,** 1845, doi:10.1029/2002GL014963.

Hagelberg, T., Shackleton, N.J., Pisias, N. & Shipboard Scientific Party, 1992. Development of composite depth sections for Sites 844 through 854, in *Proc. ODP Initial Reports,* **138**, pp. 79–85, eds Mayer, L.A., Pisias, N.G., Janecek, T.R. *et al.,* Ocean Drilling Program, College Station, TX.

Hoffman, K.A., 1992. Dipolar reversal states of the geomagnetic field and core-mantle dynamics, *Nature,* **359,** 789–794.

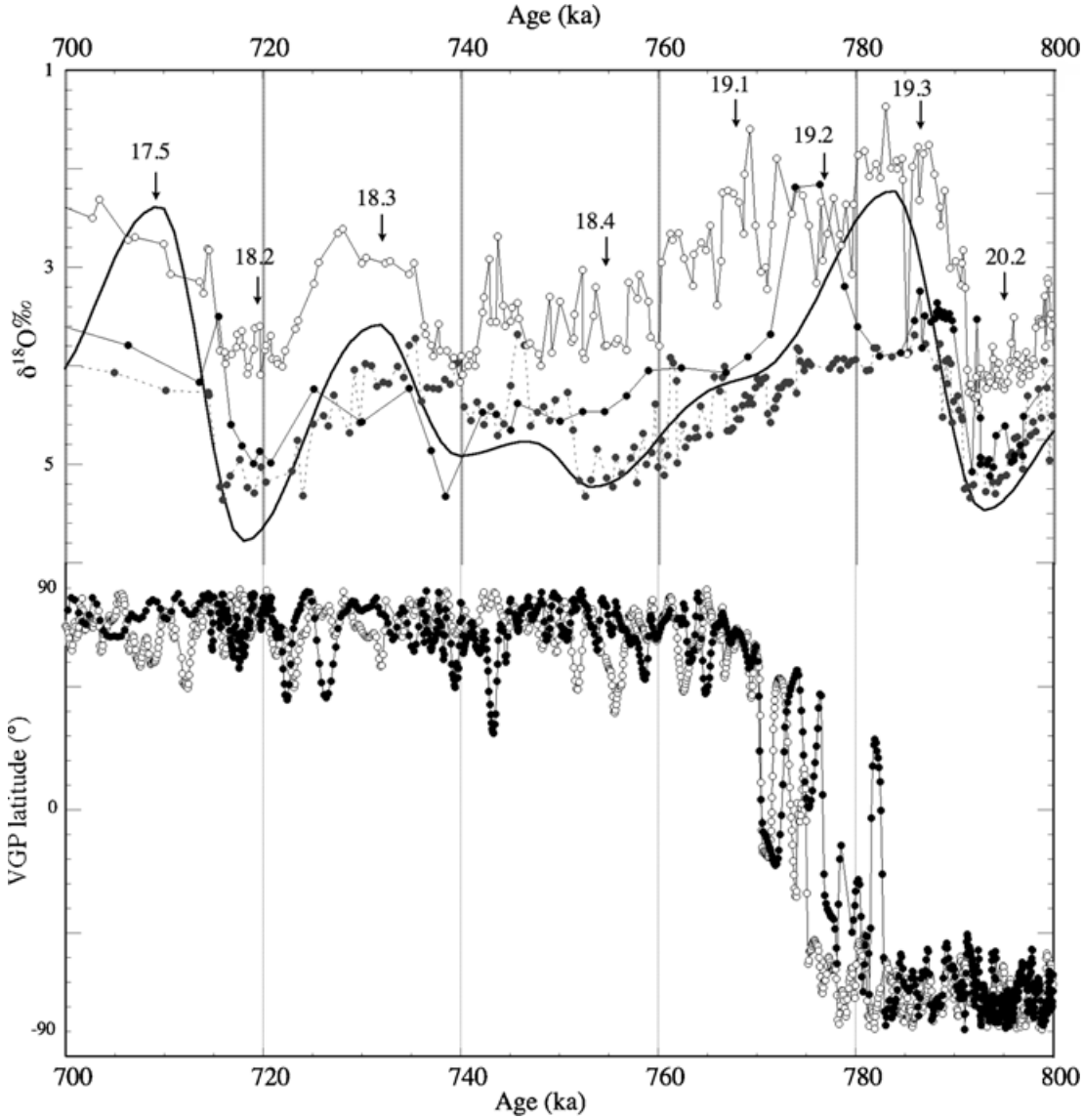

Figure 14. The MatuyamaBrunhes boundary. Top: site 984 planktonic δ^{18}O (solid line, open symbols) and benthic δ^{18}O (solid line, closed symbols) and site 983 benthic δ^{18}O (dashed line, closed symbol) compared with the Ice Volume Model (solid line). Isotopic substage nomenclature after Bassinot *et al.* (1994). Bottom: virtual geomagnetic polar (VGP) latitudes for component magnetizations computed from u-channel data from the composite section at sites 984 (closed symbols) and 983 (open symbols).

Hoffman, K.A., 2000. Temporal aspects of the last reversal of the Earth's magnetic field, *Phil. Trans. R. Soc. Lond.,* A, **358,** 1181–1190.

Hoffman, K.A. & Singer, B.S., 2004. Regionally recurrent paleomagnetic transitional fields and mantle processes, in *Timescales of the Paleomagnetic Field,* AGU Geophysical Monograph, eds Channell, J.E.T., Kent, D.V., Lowrie, W. & Meert, J., American Geophysical Union, Washington, DC, in press.

Imbrie, J. & Imbrie, J.Z., 1980. Modeling the climatic response to orbital variations, *Science,* **207,** 943–953.

King, J.W., Banerjee, S.K. & Marvin, J., 1983. A new rock-magnetic approach to selecting sediments for geomagnetic paleointensity studies: application to paleointensity for the last 4000 years, *J. geophys. Res.,* **88,** 5911–5921.

Kirschvink, J.L., 1980. The least squares lines and plane analysis of paleomagnetic data, *Geophys. J. R. astr. Soc.,* **62,** 699–718.

Kleiven, H.F., Jansen, E., Curry, W.B., Hodell, D.A. & Venz, K., 2003. Atlantic Ocean thermohaline circulation changes on orbital to suborbital timescales during the mid-Pleistocene, *Paleoceanography,* **18,** 1008, doi:10.1029/2001PA000629.

Laj, C., Mazaud, A., Weeks, R., Fuller, M. & Herrero-Bervera, E., 1991. Geomagnetic reversal paths, *Nature,* **351,** 447

Laj, C., Kissel, C., Mazaud, A., Channell, J.E.T. & Beer, J., 2000. North Atlantic Paleointensity Stack since 75 ka (NAPIS-75) and the duration of the Laschamp event, *Phil. Trans. R. Soc. Lond.,* A, **358,** 1009–1025.

Love, J.J. & Mazaud, A., 1997. A database for the Matuyama–Brunhes magnetic reversal, *Phys. Earth planet. Int.,* **103,** 207–245.

Lund, S.P., Williams, T., Acton, G.D., Clement, B. & Okada, M., 2001. Brunhes chron magnetic field excursions from Leg 172 sediments, in *Proc. ODP Sci. Results, 172,* pp. 1–18, eds Keigwin, L.D., Rio, D., Acton, G.D. & Arnold, E., Ocean Drilling Program, College Station TX.

Mazaud, A. & Channell, J.E.T., 1999. The top Olduvai polarity transition at ODP Site 983 (Iceland Basin), *Earth planet. Sci. Lett.,* **166,** 1–13.

McIntyre, K., Ravelo, A.C. & Delaney, M.L., 1999. North Atlantic intermediate waters in the late Pliocene to early Pleistocene, *Paleoceanography,* **14,** 324–335.

McManus, J., Oppo, D.W. & Cullen, J.L., 1999. A 0.5-million-year record of millennial-scale climate variability in the North Atlantic, *Science,* **283,** 971–974.

Meynadier, L., Valet, J.-P., Bassinot, C., Shackleton, N.J. & Guyodo, Y., 1994. Asymmetrical saw-tooth pattern of the geomagnetic field intensity from equatorial sediments in the Pacific and Indian Oceans, *Earth planet. Sci. Lett.,* **126,** 109–127.

Oda, H., Shibuya, H. & Hsu, V., 2000. Paleomagnetic records of the Brunhes/Matuyama polarity transition from ODP leg 124 (Celebes and Sulu seas), *Geophys. J. Int.,* **142,** 319–338.

Oppo, D.W., McManus, J.F. & Cullen, J.L., 1998. Abrupt climate events 500 000–340 000 years ago: evidence from subpolar North Atlantic sediments, *Science,* **279,** 1335–1338.

Ortiz, J., Mix, A., Harris, S. & O'Connell, S., 1999. Diffuse spectral reflectance as a proxy for percent carbonate content in north Atlantic sediments, *Paleoceanography,* **14,** 171–186.

Paillard, D., Labeyrie, L. & Yiou, P., 1996. Macintosh program performs time-series analysis., *EOS, Trans. Am. geophys. Un.,* **77,** 379.

Quidelleur, X., Gillot, P.Y., Carlut, J. & Courtillot, V., 1999. Link between excursions and paleointensity inferred from abnormal field directions recorded at La Palma around 600 ka, *Earth planet. Sci. Lett.,* **168,** 233–242.

Raymo, M.E., Ganley, K., Carter, S., Oppo, D.W. & McManus, J., 1998. Millennial-scale climate instability during the early Pleistocene epoch, *Nature,* **392,** 699–702.

Roberts, A.P., Winklhofer, M., Liang, W.-T. & Horng, C.-S., 2003. Testing the hypothesis of orbital (eccentricity) influence on Earth's magnetic field, *Earth planet. Sci. Lett.,* **216,** 187–192.

Sarna-Wojcicki, A.M., Pringle, M.S. & Wijbrans, J., 2000. New $^{40}Ar/^{39}Ar$ age of the Bishop Tuff from multiple sites and sediment rate calibration for the Matuyama–Brunhes boundary, *J. geophys. Res.,* **105,** 21 431–21 443.

Shackleton, N.J., Berger, A. & Peltier, W.R., 1990. An alternative astronomical calibration of the lower Pleistocene timescale based on ODP Site 677, *Trans. R. Soc. Edinburgh: Earth Sci.,* **81,** 251–261.

Shackleton, N.J., Crowhurst, S., Hagelberg, T., Pisias, N.G. & Schneider, D.A., 1995. A new Late Neogene time scale: application to Leg 138 sites, in *Proc. ODP, Sci. Results,* **138**, pp. 73–101, eds Pisias, N.G., Mayer, L.A., Janecek, T.R., Palmer-Julson, A. & van Andel, T.H., Ocean Drilling Program, College Station, TX.

Shipboard Scientific Party, 1996. Site 984, in *Proc. ODP, Initial Reports,* **162**, pp. 169–222, eds Jansen, E., Raymo, M., Blum, P. *et al.,* Ocean Drilling Program, College Station, TX.

Singer, B.S. & Pringle, M.S., 1996. Age and duration of the Matuyama–Brunhes geomagnetic polarity reversal from $^{40}Ar/^{39}Ar$ incremental heating analysis of lavas, *Earth planet. Sci. Lett.,* **139,** 47–61.

Stoner, J.S., Laj, C., Channell, J.E.T. & Kissel, C., 2002. South Atlantic (SAPIS) and North Atlantic (NAPIS) geomagnetic paleointensity stacks (0–80 ka): implications for inter-hemispheric correlation, *Quaternary Sci. Rev.,* **21,** 1141–1151.

Tauxe, L., 1993. Sedimentary records of relative paleointensity of the geomagnetic field: theory and practice, *Rev. Geophys.,* **31,** 319–354.

Tauxe, L., LaBrecque, J.L., Dodson, R. & Fuller, M., 1983. U-channels—a new technique for paleomagnetic analysis of hydraulic piston cores, *EOS, Trans. Am. geophys. Un.,* **64,** 219.

Tauxe, L., Herbert, T., Shackleton, N.J. & Kok, Y.S., 1996. Astronomical calibration of the Matuyama–Brunhes boundary: consequences for the magnetic remanence acquisition in marine carbonates and Asian loess sequences, *Earth planet. Sci. Lett.,* **140,** 133–146.

Valet, J.P. & Meynadier, L., 1993. Geomagnetic field intensity and reversals during the past four million years, *Nature,* **366,** 234–238.

Valet, J.P., Tauxe, L. & Clement, B.M., 1989. Equatorial and mid-latitude records of the last geomagnetic reversal from the Atlantic ocean, *Earth planet. Sci. Lett.,* **94,** 371–384.

Venz, K.A., Hodell, D.A., Stanton, C. & Warnke, D.A., 1999. A 1.0 Myr record of glacial North Atlantic intermediate water variability from ODP Site 982 in the northeast Atlantic, *Paleoceanography,* **14,** 42–52.

Weeks, R., Laj, C., Endignoux, L., Fuller, M., Roberts, A., Manganne, R., Blanchard, E. & Goree, W., 1993. Improvements in long-core measurement techniques: applications in palaeomagnetism and palaeoceanography, *Geophys. J. Int.,* **114,** 651–662.

Yamazaki, T., 1999. Relative paleointensity of the geomagnetic field during the Brunhes Chron recorded in the North Pacific deep-sea sediment cores: orbital influence?, *Earth planet. Sci. Lett.,* **169,** 23–35.

Yamazaki, T. & Oda, H., 2002. Orbital influence on Earth's magnetic field: 100,000-year periodicity in inclination, *Science,* **295,** 2435–2438.

Yang, Z., Clement, B.M., Acton, G.D., Lund, S.P., Okada, M. & Williams, T., 2001. Records of the Cobb Mountain Subchron from the Bermuda Rise (ODP Leg 172), *Earth planet. Sci. Lett.,* **193,** 303–313.